JOURNAL OF GEOPHYSICAL RESEARCH, VOL. 115, G03005, doi:10.1029/2009JG000972, 2010



# Analysis of airborne LiDAR surveys to quantify the characteristic morphologies of northern forested wetlands

Murray C. Richardson,[1,2] Carl P. J. Mitchell,[3] Brian A. Branfireun,[1] and Randall K. Kolka[4]

Received 11 February 2009; revised 20 November 2009; accepted 17 February 2010; published 16 July 2010.

[1] A new technique for quantifying the geomorphic form of northern forested wetlands from airborne LiDAR surveys is introduced, demonstrating the unprecedented ability to characterize the geomorphic form of northern forested wetlands using high-resolution digital topography. Two quantitative indices are presented, including the lagg width index (LWI) which objectively quantifies the lagg width, and the lateral slope index (LSI) which is a proxy measurement for the dome shape or convexity of the wetland ground surface. For 14 forested wetlands in central Ontario, Canada, northwestern Ontario, Canada, and northern Minnesota, United States, these indices were systematically correlated to metrics of topographic setting computed from LiDAR digital elevation models. In particular, these indices were strongly correlated with a Peatland Topographic Index (PTI, $r^2 = 0.58$ and $r^2 = 0.64$, respectively, $p <= 0.001$) describing the relative influence of upslope contributing area on the hydrology and biogeochemistry of individual wetlands. The relationship between PTI and the LWI and LSI indices was interpreted as geomorphic evolution in response to the spatially varying influence of upslope runoff on subsurface hydrochemistry. Spatial patterns of near-surface pore water chemistry were consistent with this interpretation. Specifically, at four wetland sites sampled extensively for pore water chemistry, the mean and variance of near-surface pore water methylmercury (MeHg) concentrations were higher within the zone of enhanced upland-wetland interactions, as inferred from the LiDAR-derived LWI estimates. Use of LiDAR surveys to measure subtle topographic gradients within wetlands may therefore help quantify the influence of upland-wetland interactions on biogeochemical cycling and export in northern forested landscapes.

**Citation:** Richardson, M. C., C. P. J. Mitchell, B. A. Branfireun, and R. K. Kolka (2010), Analysis of airborne LiDAR surveys to quantify the characteristic morphologies of northern forested wetlands, *J. Geophys. Res.*, *115*, G03005, doi:10.1029/2009JG000972.

## 1. Introduction

[2] Forested wetlands exert a disproportionately large influence on surface water chemistry in northern forested landscapes. For example, forested wetlands are known to be a critical source area for dissolved organic carbon (DOC) and methyl mercury (MeHg) to downstream surface waters in boreal regions [*Branfireun et al.*, 1996; *Creed et al.*, 2003; *St. Louis et al.*, 1994]. They also have the potential to delay the recovery of some Boreal headwater lakes impacted by acid deposition, due to the episodic release of sulfate from peat pore waters following prolonged periods of drought [*Devito and Hill*, 1999]. Wetlands are even believed to magnify watershed sensitivity to atmospheric inorganic mercury pollution, a phenomenon that is intricately tied to carbon and sulfur cycling [*Munthe et al.*, 2007].

[3] Despite these important biogeochemical functions, research has shown that not all wetlands are similar with respect to their ability to modify downstream surface water chemistry, and frequently these functional differences are caused by variability in their underlying hydrology [*Devito and Hill*, 1999]. This confounds our ability to characterize wetlands on the basis of their prevailing biogeochemical functional characteristics. *Devito et al.* [1999] found that hydrogeomorphic setting is a first-order control on sulfur retention and mobilization in the Muskoka-Haliburton region of south central Ontario. Resulting from these findings was a predictive landscape-scale empirical model that could explain a significant amount of the spatial and temporal dynamics of stream water sulfate concentrations in this

[1]Department of Geography, University of Toronto at Mississauga, Mississauga, Ontario, Canada.
[2]Now at Department of Geography and Environmental Studies, Carleton University, Ottawa, Ontario, Canada.
[3]Department of Physical and Environmental Sciences, University of Toronto at Scarborough, Toronto, Ontario, Canada.
[4]Northern Research Station, Forest Service, U.S. Department of Agriculture, Grand Rapids, Minnesota, USA.


0148-0227/10/2009JG000972

landscape, on the basis of wetland area and surficial geology information alone. Similarly, *St. Louis et al.* [1994] found significant differences in MeHg export from wetlands in different topographic settings at the Experimental Lakes Area in northwestern Ontario. However, they did not extend these findings to a broader landscape scale. To advance watershed management in northern forested landscapes and to better predict the influence of wetlands on water quality in these regions, new techniques are required that can help distinguish forested wetlands on the basis of their prevailing hydrological and biogeochemical characteristics.

[4] One potential strategy for inferring functional characteristics (e.g., MeHg source strength) of northern forested wetlands is through quantitative analysis of their geomorphic form. *Damman* [1986] originally outlined major classes of peatland types and characteristic morphologies as a function of their hydrologic characteristics. The "lagg" represents the mixing zone of wetland and upland runoff end-members, frequently associated with distinct subsurface chemistry and vegetation communities [*Damman*, 1986; *Urban et al.*, 1989; *Waddington et al.*, 2005]. Geomorphic characteristics such as surface convexity and the marginal "lagg" area influenced by nutrient-laden upland runoff provide important insight into the dominant sources of water and the likely hydrochemical conditions within the subsurface environment. Northern forested wetlands, which typically fall somewhere between ombrogenous and topogenous wetland classes due to the varying influence of upslope runoff, often exhibit a well defined lagg area that is generally wetter and more minerotrophic compared to the raised, central dome. Laggs are therefore a unique and biogeochemically significant geomorphic feature in northern forested landscapes.

[5] Lagg areas have been identified as important source areas of dissolved organic carbon (DOC), inorganic mercury (Hg) and MeHg [*Kolka et al.*, 2001; *Mitchell et al.*, 2008b; *Schiff et al.*, 1998]. *Mitchell et al.* [2008a] demonstrated that for certain chemical species, most notably MeHg, the proportion of a wetland's surface area that actively influences biogeochemical transformations and net MeHg production is limited primarily to its lagg areas. They attributed this spatially discrete, biogeochemical "hot spot" to the interaction between upslope runoff and wetland subsurface redox conditions, consistent with the conceptual framework put forth by *McClain et al.* [2003]. Topographic setting is therefore likely to influence MeHg source-strength potential of wetlands through the delivery of labile DOC and oxidized nutrients to sites of MeHg production in anaerobic wetland sediments. Quantitative analysis of the geomorphic form and topographic setting of forested wetlands may provide a predictive framework for quantifying the aggregated effects of biogeochemical hot spots at the landscape scale [*Richardson et al.*, 2007] such as production and export of MeHg from discrete locations within the landscape.

[6] With the widespread availability of digital topographic data, digital terrain analysis (DTA) has become commonplace in hydrological research, watershed modeling and predictive soil mapping [e.g., *Jencso et al.*, 2009; *McGlynn and Seibert*, 2003; *Scull et al.*, 2003]. DTA is also commonly used to examine the influence of topographic variability on carbon and nitrogen cycling in forested watersheds. The increasing use of DTA in these different research disciplines reflects the growing recognition that landscapes can be stratified on the basis of topographically defined functional units within which uniform hydrological and biogeochemical conditions can more reasonably be assumed. For example, *Webster et al.* [2008] used a spatial partitioning scheme based on fuzzy classification with digital elevation model (DEM) derivatives to improve catchment-scale aggregation of carbon dioxide efflux from soils. Similarly, *Florinsky et al.* [2004] used DTA to stratify the landscape into functional areas related to denitrification potential. *Creed et al.* [2003] used a stochastic depression filling algorithm to delineate cryptic wetlands in the Algoma Highlands of central Ontario, significantly improving watershed regression models of DOC export. *Richardson et al.* [2009] used an edge detection approach to delineate wetlands in the Muskoka-Haliburton region of south central Ontario, and were able to distinguish true wetlands from nonwetland depressional areas on the basis of topographic metrics used as proxies of hydraulic residence time in discrete landscape units. In many of the above examples DTA routines were conducted on high-resolution (≤5 m pixel dimensions) LiDAR DEMs. The increasing availability of LiDAR data is therefore an important technological development that is dramatically improving our ability to investigate topographic controls on landscape hydrology and soil biogeochemical dynamics. However, it should be noted that some traditional spatial partitioning techniques are problematic when applied to high-resolution digital elevation models [*MacMillan et al.*, 2003].

[7] Given the very fine topographic detail captured in LiDAR surveys, there is ample opportunity to develop new DTA techniques that can be used to infer functional characteristics of forested wetlands from their topographic setting and geomorphic characteristics. Only recently have researchers begun to use DTA to examine the geomorphology of wetland environments, but these applications have primarily been in relation to large wetland complexes such as northern peatlands and deltaic wetland environments. For example, *Sonnentag et al.* [2008] used local polynomial interpolation to characterize the dome shape of Mer Bleu Bog in Ottawa, Ontario, Canada using a 10 m resolution DEM. This was found to significantly improve the parameterization and accuracy of a fully distributed hydrologic simulation model. *Toyra and Pietroniro* [2005] used a LiDAR DEM to detect subtle topographic differences (on the order of 0.5–2 m), between wetland feature types having distinct vegetation communities, in the Peace-Athabasca Delta, a large wetland complex in northeastern Alberta, Canada. Recently, *Jones et al.* [2008] presented a new DTA technique for quantifying hydrologic connectivity among morphologic units in a large floodplain wetland complex. These studies clearly demonstrate that the resolution and accuracy of currently available DEMs has reached a level of detail that is sufficient for examining subtle topographic gradients within wetlands. Nevertheless, DTA has yet to be applied to assess geomorphic characteristics of small, forested wetlands, nor has it been used to help explain spatial patterns of subsurface biogeochemistry at the wetland scale.

[8] Accordingly, this study examined the influence of topographic setting on wetland geomorphology and subsurface biogeochemistry in northern forested wetlands

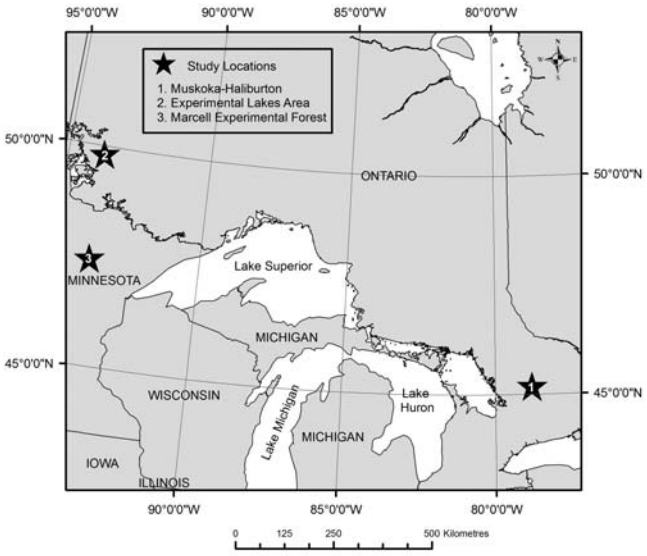


**Figure 1.** Locations of the three study regions in south central Ontario, northwestern Ontario, and north central Minnesota.

through a combined analysis of airborne LiDAR topography, and previously published pore water chemistry data [*Mitchell et al.*, 2008b]. The research objectives were threefold; (1) to conduct an accuracy assessment of LiDAR ground return elevations in forested wetlands and determine the precision with which geomorphic gradients within such wetlands can be quantified; (2) to develop quantitative metrics of lagg geomorphology and surface convexity from LiDAR topography and to relate them to geomorphic metrics describing the topographic setting of individual wetlands; and (3) to assess the potential correlation between spatial variability in pore water MeHg concentrations and LiDAR-derived indices of lagg geomorphology at four intensively studied wetland sites in northwestern Ontario and northern Minnesota.

## 2. Site Descriptions

[9] This study spanned three physiographic regions including the Muskoka-Haliburton area of south central Ontario, near Dorset (45°14′N, 78°54′W), the Experimental Lakes Area (ELA, 49°40′N, 93°43′W) in northwestern Ontario, near Kenora, and the Marcell Experimental Forest (MEF, 47°53′N, 93°46′W) in north central Minnesota, near Grand Rapids (Figure 1). The Muskoka-Haliburton sites fall within lake basins and gauged subwatersheds that form part of a long-term, small catchment monitoring network maintained by the Ontario Ministry of Natural Resources. A similar network is maintained at the ELA by the Department of Fisheries and Oceans and Environment Canada. The MEF is an experimental forest operated by the United States Department of Agriculture Forest Service. In total, 14 forested wetlands greater than 2ha were chosen for this study: 3 from MEF, 3 from ELA and 8 from the Muskoka-Haliburton region. Geochemical data for this study was taken from *Mitchell et al.* [2008b], who sampled extensively for near-surface pore water chemistry at 4 of these 14 sites, 2 of which were at the ELA and 2 of which were at the MEF.

[10] At the Ontario sites, bedrock governs the occurrence of topographically defined features in the landscape, with dry uplands typically occurring where slopes exceed 1–2% [*Richardson et al.*, 2009] and lakes, beaver ponds, and wetlands typically occurring in bedrock depressions. Upland areas in the Muskoka-Haliburton region are typical of glaciated, boreal shield landscapes (thin till, exposed bedrock ridges). Previous research in this area has shown that the extent of upland-wetland hydrologic connectivity is dictated by till depth and the temporal persistence of perched, shallow groundwater tables during dry summer periods (i.e., thinner till deposits result in less persistent upland-wetland hydrologic connectivity due to reduced water storage capacity of hillslopes) [*Devito and Hill*, 1997]. At ELA, where bedrock also controls the formation of topographic features, the landscape is dominated more significantly by exposed bedrock ridges, with some pockets of very thin soils throughout the upland areas. Upland-wetland hydrologic connectivity is likely similar to the shallow-till sites in the Muskoka-Haliburton region. In contrast to both of the Ontario sites, MEF is in a recessional moraine landscape with deep overburden on the order 40–55 m deep and a significant regional groundwater system. The wetland sites at MEF chosen for this study however, have perched water tables that are meters above the influence of the regional water table (we did not analyze fen wetlands with known connections to the regional aquifer system). Despite the deep glacial drifts at the Minnesota sites, the research catchments are characterized by a low-permeability sandy clay or silt layer at 45–60 cm below the ground surface in the uplands. Importantly, previous research has demonstrated that most runoff from the uplands into the wetlands occurs as either near surface runoff through the organic horizon or as interflow at the interface between the sandy loam layer and this relatively impermeable clay/silt horizon [*Timmons et al.*, 1977]. Given the relatively thin soil mantle, the groundwater in the MEF uplands is only an ephemeral, shallow perched system that varies throughout the year and may be absent altogether in mid to late summer. Therefore subsurface hydrologic connectivity between uplands and wetlands at MEF is also very likely transient throughout the summer period depending on antecedent wetness conditions. It is therefore well established that all of the wetlands chosen for this study are dominated by hydrologic inputs from precipitation and transient shallow-groundwater flow systems, and unaffected by regional groundwater influences.

[11] The three study sites have similar climatic characteristics, with the Muskoka-Haliburton sites being somewhat wetter than both the MEF and the ELA sites. Climate at MEF is subhumid continental, with average annual January and July air temperatures of −14°C and 19°C, respectively. Long-term mean annual precipitation is 762 mm, 25% of which falls as snow. Climate at the ELA is cold temperate continental, with mean January and July air temperatures of −17°C and 20°C, respectively. Long-term mean annual precipitation is 690 mm, 27% of which falls as snow (M. Lyng and K. Beaty, unpublished report, 2010). In the Muskoka-Haliburton region, climate is humid continental, with average annual January and July air temperatures of −10°C and 16°C, respectively [*Yao and Deveau*, 2009].

Long-term mean annual precipitation is 1008 mm, based on data from the closest meteorological station maintained by the Ontario Ministry of the Environment Dorset Environmental Science.

## 3. Methods

### 3.1. LiDAR Acquisition

[12] LiDAR surveys were completed in all three study regions by various service providers in either 2005 or 2006. The spatial coverages at the Muskoka-Haliburton, MEF, and ELA sites were approximately 1600, 1330, and 1840 ha, respectively. Each of the LiDAR service providers classified the raw data into ground and vegetation returns using proprietary techniques, and shipped the data in tiled, x, y, z data files. Only the classified ground returns were used in this study. The point density of ground returns varied somewhat due to the different LiDAR instruments used, and possibly also due to different instrument settings, flight specifications and forest canopy characteristics. At ELA, average point density was 0.3 points/$m^2$. At MEF and the Muskoka-Haliburton sites, average point density was 0.4 points/$m^2$.

### 3.2. Multiscale Accuracy Assessment of LiDAR-Derived Ground Surface Elevations

#### 3.2.1. Field Survey

[13] A Topcon Systems Inc. HiPer Ga real time kinematic (RTK) global positioning system was used to collect over 400 high-precision (5–10 mm vertical accuracy) ground surface elevations along two transects in the 2.2 ha Plastic Swamp wetland at the PC1 research catchment in the Muskoka-Haliburton region. This site was chosen because there are numerous boardwalks that facilitate walking throughout the wetland site. The site is also characterized by a variety of vegetation types including white cedar, black spruce, birch, maple and an understory primarily composed of alder. A well-developed layer of sphagnum blankets the ground surface and a hummock-hollow topography has developed throughout [*Devito and Hill*, 1997]. Measurements along two, 4 m-wide transects (120 m and 180 m long, respectively) were collected with an approximately uniform, average density of 0.3 points per square meter. A 10 cm radius disk was fixed to the bottom of the range pole to minimize sinking of the GPS into the compressible peat surface, which would cause a downward bias in the surveyed elevations. The GPS unit computes and reports an estimate of vertical precision during data collection which is primarily a function of satellite configuration and availability, and length of occupation at a point. In particular, as occupation time increases, the estimated precision improves. During the surveying campaigns, all elevation points were collected with a minimum precision of 10 mm, which was well below the range of natural topographic variability in wetlands as well as the vertical precision of individual LiDAR ground returns. Typically the reported vertical accuracies of individual occupations reached as low as 2–5 mm.

#### 3.2.2. Analysis

[14] The absolute accuracy of LiDAR ground returns in wetland areas with low shrubs have been reported to be on the order of ±12 cm (1 standard deviation) [*Hopkinson et al.*, 2005] considerably poorer than 7–8 cm, which is typically stated by LiDAR service providers. Many of the forested wetlands at the study sites support understory vegetation, and an error margin of ±12 cm could jeopardize the ability to quantify geomorphic gradients of a similar magnitude. Therefore an accuracy assessment of LiDAR-derived topography in forested wetlands was conducted.

[15] It is important to note that the characteristic morphology assessment was based on an analysis of large populations of LiDAR ground returns (on the order of n = 100–1000) within consecutive buffer zones rather than using a gridded DEM interpolated from the ground returns (section 3.3). Therefore conducting an accuracy assessment of individual ground returns or an interpolated DEM, as compared to surveyed spot elevations, would not necessarily reflect the true accuracy of the characteristic geomorphology derivation. A less stringent accuracy assessment was thus required to reflect the fact that the geomorphic indices describing wetland surface morphology were derived by assessing the central tendency of large populations of LiDAR ground returns within spatially discrete zones of the wetland. To this end, a multiscale accuracy assessment was conducted to gain insight into the degree of accuracy that could be expected for LiDAR ground surface elevations within forested wetlands as a function of the scale of observation. Five scales of analysis were used, representing increasing levels of spatial aggregation. Agreement between LiDAR-derived versus surveyed ground surface topography at all analysis scales were assessed on the basis of root mean square error (RMSE) and the correlation coefficient (r). For levels 1–3, LiDAR-derived versus survey-derived elevations along the 120 m lateral transect were also compared visually by plotting the elevation profiles together for each scenario. The analysis details for each level of assessment were as follows:

##### 3.2.2.1. Accuracy Assessment Level 1: Nearest-Neighbor Comparison

[16] Elevations of individual LiDAR ground returns were assessed relative to the closest field surveyed spot height elevation. Only points that were within 30 cm of one another were included in the analysis.

##### 3.2.2.2. Accuracy Assessment Levels 2 and 3: IDW Interpolation

[17] For level 2, surveyed spot-height elevations were compared to the nearest value in a 2 m grid cell resolution DEM derived from the LiDAR ground returns using Inverse Distance Weighted (IDW) interpolation with maximum number of neighbors set to 5 and a power of 1. For level 3, spot heights were also interpolated at 2 m intervals (to simulate a DEM interpolation from surveyed spot heights along the transects), using the same IDW parameters as above. The values interpolated from LiDAR ground returns versus surveyed spot heights were subsequently compared.

##### 3.2.2.3. Accuracy Assessment Levels 4 and 5: Local Cluster Means

[18] Mean elevations in spatially contiguous clusters of LiDAR ground returns and surveyed spot heights were computed and compared for two different cluster sizes. The surveyed spot heights were used as seeds to derive the spatial clusters. At each spot height the mean elevations of all LiDAR ground returns and surveyed spots heights were computed for the nearest 10 (level 4) and 25 (level 5) observations, and these were used to compute the accuracy

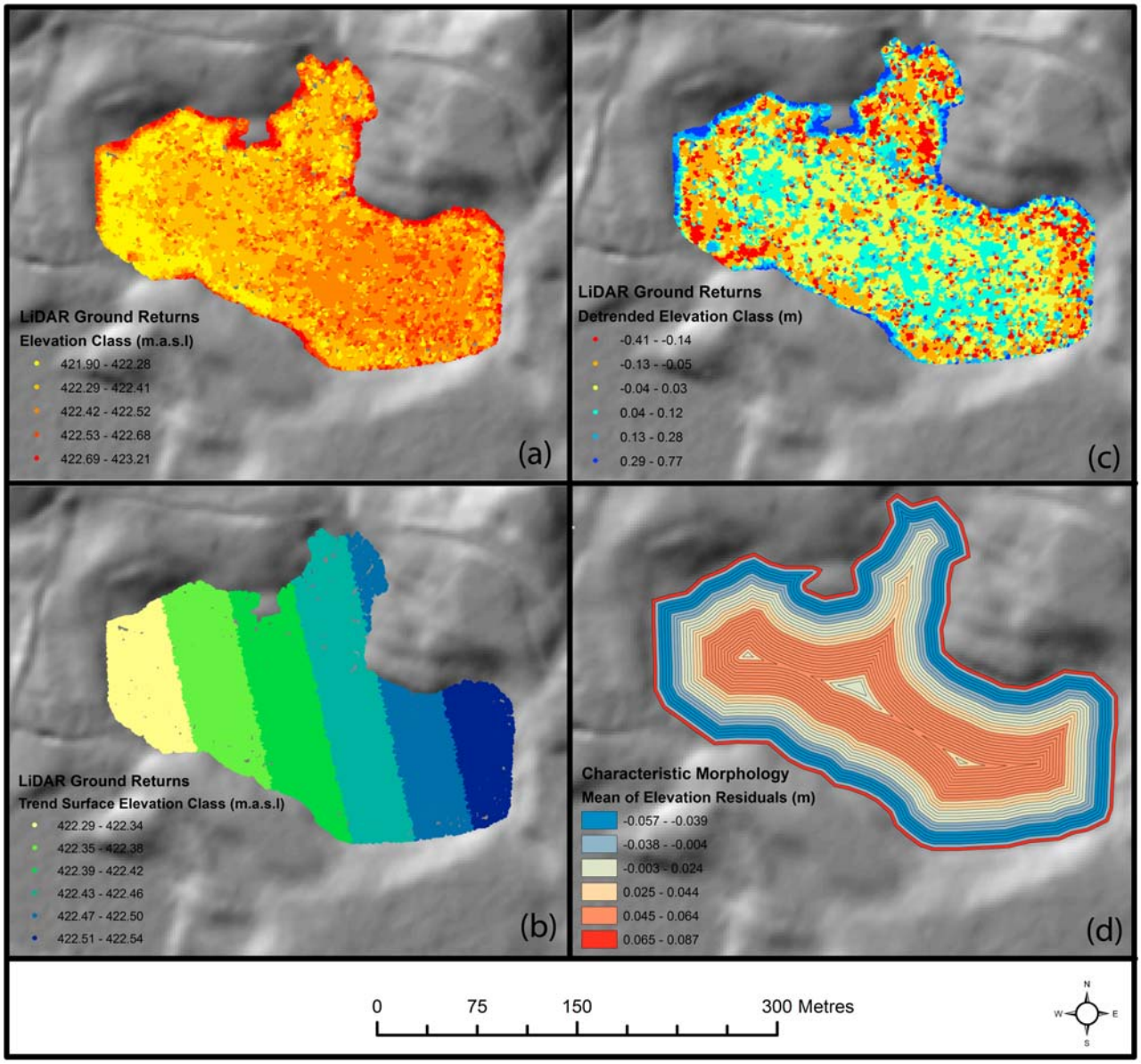


**Figure 2.** Elements of the characteristic morphology analysis illustrated for S2 wetland at MEF. (a) LiDAR ground returns are extracted for the wetland (close to 30,000 individual points in this case); (b) a trend surface is fit to the LiDAR ground returns, and each ground return is assigned the trend surface elevation at that point; (c) the trend surface elevation is subtracted from the ground surface elevation to produce detrended elevation residuals; (d) the median elevation of the residuals is computed for 2 m wide buffer strips extending from the wetland margin to the wetland center. The result of this entire analysis is a box plot such as the one seen in Figure 3.

statistics for each level. We consider levels 4 and 5 to be the most relevant scales of analysis for this study since the characteristic morphology indices were derived from the statistical distribution of large LiDAR ground return populations within spatially discrete zones of the wetlands.

### 3.3. Quantifying Characteristic Morphologies of Forested Wetlands Using LiDAR Ground Returns

[19] All forested wetlands in the three study regions were delineated from 1 m interpolated digital elevation models using a newly developed, hydrogeomorphic edge detection and thresholding routine [*Richardson et al.*, 2009]. In total, 14 wetlands greater than 2 ha were analyzed for their characteristic morphologies based on a residual analysis approach using the classified LiDAR ground returns. The ground returns were used instead of an interpolated DEM because they provide a better indication of the distribution of observed elevation values, as influenced by both natural variability and measurement error in the LiDAR system. Typically there were between 10 and 40 thousand LiDAR ground returns per wetland site that were used in the analyses. For each wetland, a first- to fourth-order polynomial trend surface was fit to the entire population of LiDAR ground returns falling within its perimeter (Figures 2a and 2b). This

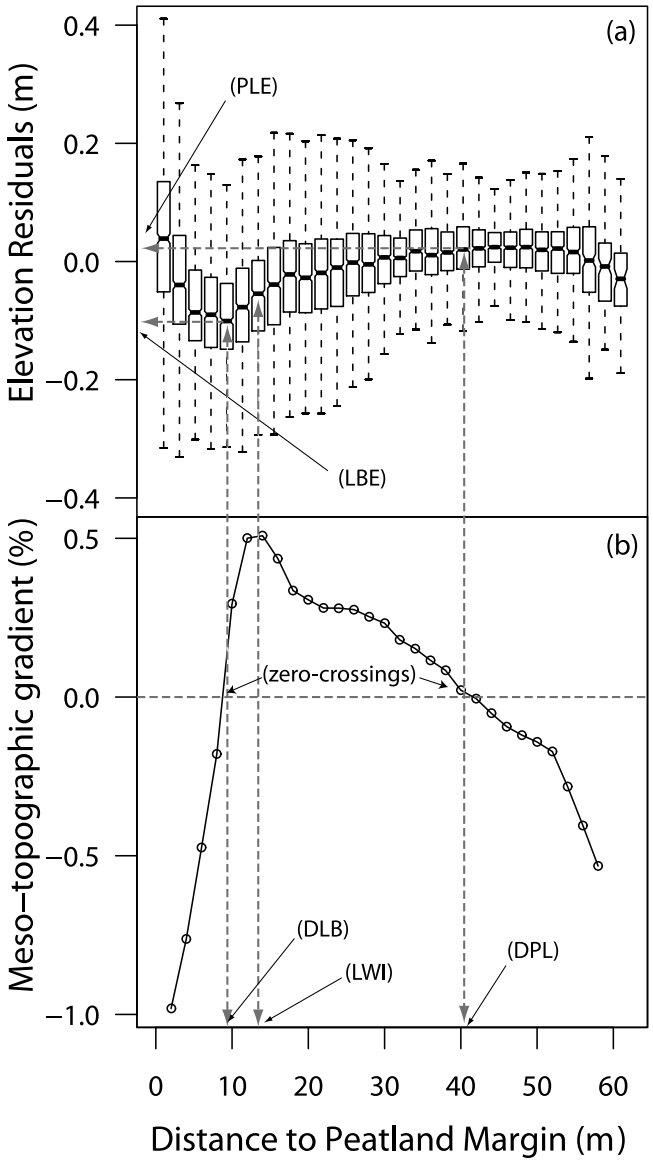


**Figure 3.** (a) The characteristic morphology plot for S2 bog at MEF and (b) derivation of the quantitative indices to describe it. DLB, distance to lagg bottom; LWI, lagg width index; DPL, distance to plateau; LBE, lagg bottom elevation; PLE, plateau elevation.

modeled trend surface elevation was then subtracted from the ground surface elevation at each ground return location to produce elevation residuals (Figure 2c). The residuals therefore represented the detrended ground surface topography, which were used to analyze the shape of the wetland ground surface. This was a critical step in the analysis since the downslope gradient modeled by the trend surface was often of a greater magnitude than that of the geomorphic gradients of interest, which would otherwise be difficult or impossible to quantify. In fitting the trend surface, the minimal polynomial order required to represent the wetland surface was used that could yield a satisfactorily normal distribution of elevation residuals, based on visual inspection and an assessment of the RMSE values. The distribution of elevation residuals within successive, 2 m-wide buffer strips extending from the wetland margin to wetland center (Figure 2d) were subsequently plotted as box plots for each 2 m distance class (Figure 3a). These box plots illustrate the "characteristic morphology" or the average shape of the ground surface after removal of the modeled trend surface elevations.

[20] Two principle geomorphic indices, the lagg width index (LWI) and the lateral slope index (LSI), were developed to quantitatively describe the characteristic morphology of forested wetlands. These were derived based on a gradient analysis of the elevation residual medians shown in the characteristic morphology box plot. An example for one of the studied wetlands is shown in Figure 3a. Figure 3b is a plot of the average, local surface gradient computed from the medians of each adjacent box plot in Figure 3a. Inflection points in the gradient plot are identified at zero crossings (locations where the sign of the slope changes or levels off at zero) and local maxima (locations of maximum gradient). The first inflection point is a zero crossing defining the distance to lagg bottom (DLB). The elevation at this inflection point is therefore the lagg bottom elevation (LBE). The third inflection point is also a zero crossing defining the distance to wetland plateau (DPL) and thus also the plateau elevation (PLE), where the dome shape levels off. The middle inflection point is the point of maximum slope between the lagg bottom and the plateau. The lagg width index (LWI) is defined as the distance from the wetland edge and this point of maximum slope. The lateral slope index (LSI) is defined as the average slope between the lagg bottom and the wetland plateau (Figure 3b) derived from the DLB, LBE, DPL and PLE metrics as follows:

$$\mathrm{LSI} = \frac{\mathrm{PLE} - \mathrm{LBE}}{\mathrm{DPL} - \mathrm{DLB}} \times 100 \quad (1)$$

LSI is therefore a proxy index for the degree of convexity of the wetland surface (i.e., how "domed" it is). LSI and LWI were the only two indices used for further analysis, whereas PLE, LBE, DPL and DLB were derived solely to derive LSI and LWI.

### 3.4. Quantifying the Topographic Setting of Wetlands Using LiDAR DEMs

[21] Digital terrain analysis was conducted to characterize the topographic setting of forested wetlands using a 1 m resolution gridded DEM interpolated from the LiDAR ground returns. The interpolator used was inverse distance weighting (IDW) with a power value of 1, a maximum of 4 neighbors and a search radius of 6 m at the ELA and 4 m at the Muskoka-Haliburton and MEF sites. These parameters were chosen to produce a 1 m resolution DEM without null values in areas of lower ground return density (i.e., null values were avoided by using a relatively large search radius but a low power value to avoid the "bull's-eye" or pitting effect). Conversely, in areas of higher density, a 1 m grid resolution was fine enough to capture the highest possible detail but only the closest 4 neighbors were used to avoid excessive aggregation in these areas.

[22] Various common metrics were computed including wetland area, upslope contributing area to wetland area ratio, wetland perimeter, and the mean tan $\alpha_{1m}$ index of wetland pixels, which is an indicator of local drainage

conditions as affected by downslope topography [*Hjerdt et al.*, 2004]. This index has previously been shown to be more effective for mapping wetlands compared to the use of slope measures based on the plane tangent to the elevations within a 3 × 3 moving window passed over a DEM [*Hjerdt et al.*, 2004; *Richardson et al.*, 2009]. Not only is it thought to provide a more realistic estimate of the slope of the hydraulic gradient at a point, it also helps suppress the effect of natural and random noise in LiDAR DEMs on slope estimates, which is an inherent limitation of their use in morphological analysis [*Richardson et al.*, 2009]. Composite indices derived from these metrics were upslope area to wetland area ratio, upslope area to wetland perimeter ratio, and two peatland topographic indices (PTI) akin to the $\ln(a/\tan\beta)$ index of *Beven and Kirkby* [1979] but computed at the scale of individual wetlands rather than individual pixels:

$$\mathrm{PTI}_1 = \frac{a_{upland}/a_{wetland}}{\tan\alpha_{1m}} \tag{2}$$

$$\mathrm{PTI}_2 = \frac{a_{upland}/p_{wetland}}{\tan\alpha_{1m}} \tag{3}$$

where $a_{upland}$ is the upslope area contributing to wetland, $a_{wetland}$ is the wetland area, $p_{wetland}$ is the wetland perimeter, and $\tan\alpha_{1m}$ is the mean of downslope drainage index for wetland. $\mathrm{PTI}_1$ is a dimensionless index whereas $\mathrm{PTI}_2$ has units of length. Upslope area contributing to each wetland was computed using a standard watershed delineation procedure based on the D8 (single-direction) flow routing analysis, where wetland grid cells were input as the target cells in the algorithm. The accuracy of contributing areas calculated in this way using the 1 m LiDAR DEM was assessed by comparing catchment areas for gauged watersheds in the Muskoka-Haliburton region to previously determined catchment areas based on manual surveying with a level transit and laser measuring device [*Dillon and Molot*, 1997; *Reid et al.*, 1987]. The mean absolute error of catchment areas calculated using the two different methods was 4.98%. The influence of grid cell resolution on computed upslope areas was assessed for values between 1 and 5 m. The differences in areas were negligible as a function of resolution. The influence of grid resolution on mean $\tan\alpha_d$ within all wetlands was also assessed for different values of $d$ and it was found that when $d = 1$ m, resolution had very little effect on the computed mean $\tan\alpha_d$ of the wetlands. As the $d$ parameter was increased beyond 1 m, mean $\tan\alpha_d$ values of wetlands increased systematically and were highly correlated for different $d$ specifications. Therefore the potential that the choice of $d$ could have influenced the results of this study was ruled out, and a value of 1 m was chosen since it was the least sensitive to grid cell resolution.

### 3.5. Regression Analysis Between Characteristic Morphology Indices and PTI

[23] The topographic metrics and compound indices described in section 3.4 were assessed for a possible correlation with the LWI and LSI indices describing the wetland characteristic morphologies presented in section 3.3. The models were assessed on the basis of goodness of fit and statistical significance of the fitted coefficients. This analysis was conducted to determine whether topographic setting might be a factor contributing to the geomorphic form of northern forested wetlands.

### 3.6. Pore Water Surveys and Water Chemistry

[24] Four wetland sites, S2 and S6 at MEF and L658 and L239 at ELA were sampled extensively at three different times during the growing season of 2005 (early June, early August and early October) to understand the seasonal and spatial variability of near-surface pore water chemistry. Specific details regarding the sampling and analytical methods are given by *Mitchell et al.* [2008b] but are briefly described here. At each site (georeferenced with a handheld GPS) 30–35 samples were taken at regular intervals along four to five lateral transects spanning the entire width of each wetland, following ultraclean trace metal protocols. Using a portable Teflon piezometer, peristaltic pump, and inline filtration system, pore water samples were extracted into 125 mL PETG bottles for MeHg and THg analysis, and 80 mL HDPE bottles for pH, DOC, and ion chemistry. Samples in PETG bottles were acidified in the laboratory to 0.5%, and stored at room temperature in the dark until further analysis for THg and MeHg by standard methods with cold vapor atomic fluorescence detection. Samples in the HDPE bottles were analyzed immediately for pH using a portable Orion pH meter and triode electrode. The remaining sample was refrigerated until further analysis for DOC and major ions.

### 3.7. Spatial Analysis of Pore Water Chemistry

[25] Initial scatterplots of various chemical variables including MeHg indicated marked trends in the mean and variance of the sample populations as a function of distance to the wetland margin. A spatial analysis of the pore water chemistry data was therefore conducted to determine whether spatial variability of the mean and variance of MeHg concentrations in pore waters varied systematically in relation to the LiDAR derived lagg areas. Thirty samples per date at each site were insufficient to identify clear boundaries in the MeHg data, which were inherently noisy. While the global mean MeHg concentration varied significantly at each site between sampling dates, the spatial pattern observed in the data within the wetlands did not vary significantly over time. The data were therefore standardized to z scores by date and site so that they could be pooled and analyzed for spatial trends in the absence of temporal nonstationarity. This procedure essentially removed seasonal dynamics in pore water MeHg concentrations so that the spatial patterns could be properly analyzed. To facilitate interpretation of the data and site intercomparison, at each wetland site the z scores were transformed back to MeHg concentration units based on the mean concentration and standard deviation of the pooled MeHg data (i.e., all dates). Therefore the resulting standardized and transformed data set for each wetland site had the same mean and standard deviation of the original pooled data set from all three sampling dates, but was normalized by date to facilitate the spatial analysis. Standardizing and pooling the MeHg data in this way increased the sample population to approximately 90 samples per site (3 dates × 30 sample locations, although sample sites were still limited to 30 discrete locations).

[26] Spatial nonstationarity (spatial nonuniformity in mean and variance) was assessed by computing a running mean and standard deviation for the standardized data in every 2 m buffer strip, based on an 8 m moving window from wetland edge to wetland center (as illustrated in Figure 2d). The 2 m buffer width was chosen to correspond with the characteristic morphology analysis (section 3.3). The 8 m window size was the smallest window size that could be used without resulting in an excessive number of buffer zones having an insufficient number of samples to properly compute the subsampled population mean and standard deviation. Spatial trends in the running mean and standard deviation of normalized MeHg concentrations were visually assessed for a spatial agreement with the LiDAR-derived lagg width index.

[27] All of the spatial and statistical analyses, terrain analyses and accuracy assessments described in sections 3.2–3.5 and section 3.7 were conducted using the System for Automated Geoscientific Analysis (SAGA) GIS and R statistical software [*R Development Core Team*, 2008].

## 4. Results

### 4.1. LiDAR Accuracy Assessment and Assessment of Characteristic Morphologies

[28] While the RMSE of LiDAR ground returns from open bedrock and road surfaces near the PC1 wetland was approximately 4.5 cm (data not shown) the wetland-only accuracy assessment resulted in a RMSE of almost 10 cm (accuracy assessment level 1, Figures 4a and 4b). This is significant relative to the geomorphic gradients of interest. In general, the LiDAR elevations overestimate lower-elevation features and underestimate higher-elevation features, causing a "dampening" of the true topographic variability, as seen along the 120 m lateral transect surveys (Figures 4b, 4d, and 4f). RMSE actually increased when the surveyed ground surface elevations were compared to the nearest pixel value of a 2 m DEM interpolated from the LiDAR ground returns (level 2; Figures 4c and 4d). This was expected since the interpolation significantly reduced the range of observations observed, which caused further dampening of the LiDAR topography in relation to the actual surveyed topography. The RMSE decreased significantly for the level 3 assessment, since in this case the analysis was based on 2 m resolution IDW interpolations from both the LiDAR ground returns and the surveyed ground surface elevations (Figures 4e and 4f). Therefore the range of interpolated surveyed elevations was also dampened and corresponded more closely with the interpolated LiDAR DEM elevations.

[29] RMSE of LiDAR ground topography relative to actual surveyed topography in the wetland was significantly improved when computed on the basis of local cluster means (Figure 5). These assessments compared the mean elevation of groups of 10 (level 4) and 25 (level 5) spatially contiguous LiDAR versus surveyed spot heights. Thus subsamples of spatially contiguous LiDAR ground returns can be averaged to very accurately determine the mean elevation of the ground surface over relatively small areal units. However, as in the level 2 and 3 assessments, aggregation caused a dampening of the observed topographic variability. The level 4 and 5 assessments are akin to a relatively coarse resolution IDW interpolation using a low weighting exponent (interpolated value approaches a mean value as the exponent tends toward 0). However, the use of local cluster means in level 4 and 5 assessments is conceptually more consistent with the characteristic morphology analysis presented in this study, which does not use an interpolated DEM. A positive bias of 2–5 cm away from the 1:1 line in Figure 5 at lower elevations (hollows) was attributed to slight, unavoidable compression of the peat surface due to the weight of the GPS unit.

[30] There was no obvious systematic elevation bias in relation to vegetation along the two surveyed transects despite significant variability in canopy types and understory vegetation along both of them. Leaf-out conditions had not yet reached their maximum during the time of the LiDAR survey, which was conducted in mid-May at the Muskoka-Haliburton sites. This may have reduced the possible influence of elevation biases caused by vegetation structural effects.

[31] The results of the level 5 accuracy assessment and the relatively large amount of aggregation used to derive the characteristic morphologies indicated that differences in the median elevation residuals on the order of 3 cm could be accurately quantified using the gradient analysis method shown in Figure 3b. The box plots for all 14 wetland sites analyzed exhibited systematic and consistent trends that clearly depict a raised dome shape surrounded by depressional lagg areas around the wetland margins. 95% confidence intervals for the population medians are provided as notches in the box plots and a lack of overlap between the notches of any two distance classes is strong evidence that the difference between their median values is different [*R Development Core Team*, 2008].

### 4.2. Correlation Between LiDAR-Derived Lagg Widths and Pore Water Chemistry

[32] LiDAR derived lagg widths corresponded very closely with clear breaks in the variability of pore water chemical properties in the wetlands. As an example, Figure 6 illustrates the spatial variability of pH, DOC, sulfate, THg, %THg as MeHg and MeHg at the L239 wetland in early August 2005. For reference, the LiDAR derived lagg width is also shown on each plot (18 m from wetland edge). Sulfate, pH, THg and MeHg concentrations were elevated within the LiDAR-derived lagg area. Oppositely, DOC concentrations were lowest in the lagg area and tended to increase with increasing distance from the wetland margin. In all cases at this site, variability in solute concentrations was highest in the lagg areas, decreasing with distance from the wetland margin.

[33] The standardized and transformed MeHg concentration data were clearly spatially nonstationary, with inflection points in the running mean and standard deviations corresponding to the average lagg width (Figure 7). Of the four intensively studied wetland sites, spatial variability of pore water chemistry was most strongly correlated with the LWI at the L239 peatland. In all cases however, there was a marked inflection point in the running means and standard deviations of the pore water MeHg concentrations that corresponded almost exactly to the LiDAR derived LWI (Figure 7). In general, the trends in the scatterplots were similar to those shown in Figure 6 for the L239 wetland, with some deviations. In all cases, there was a clear decrease

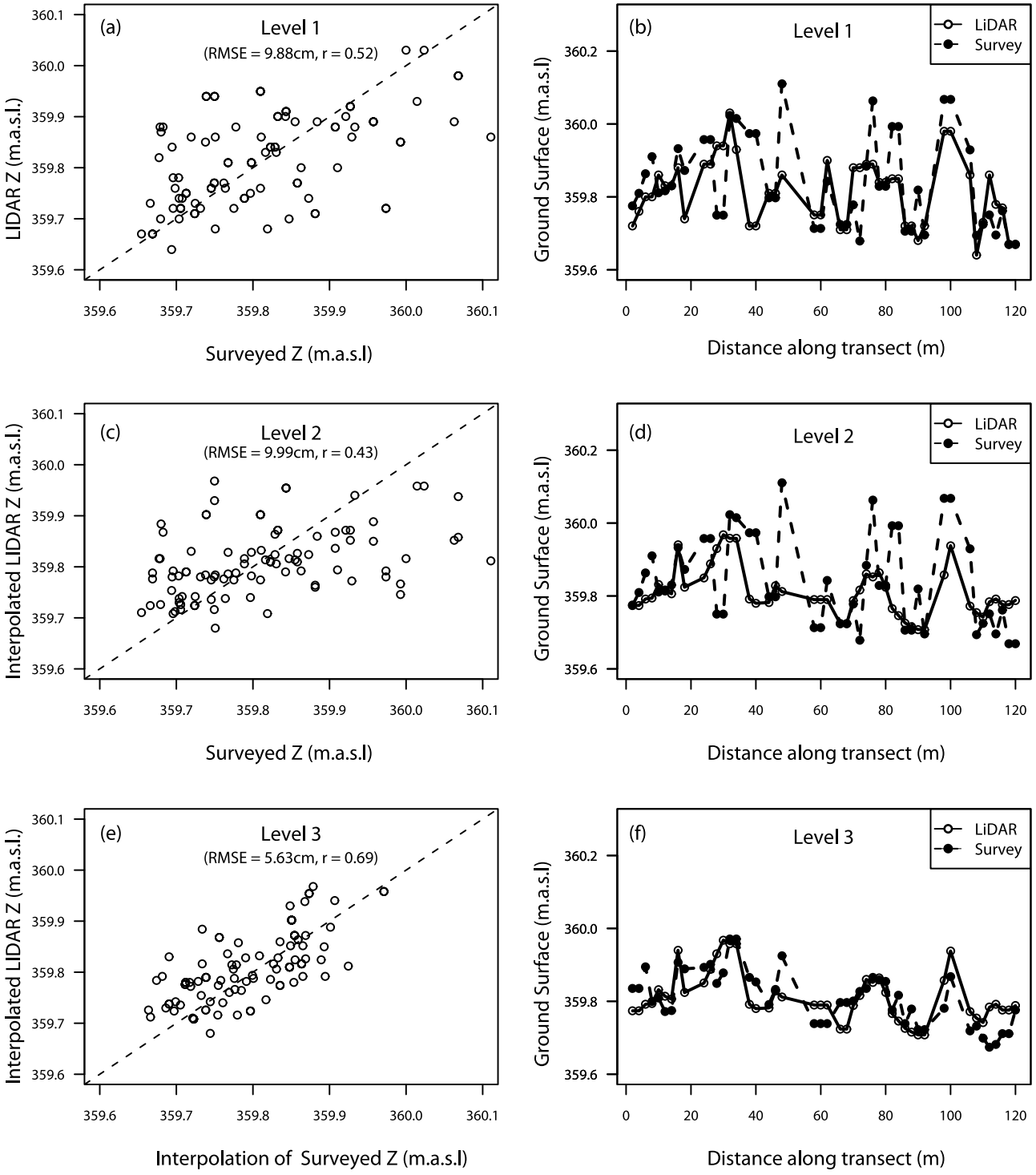


**Figure 4.** Results of LiDAR accuracy assessment for PC1 wetland in the Muskoka-Haliburton regions (levels 1–3). (left) Scatterplots comparing the LiDAR-derived versus surveyed elevations for each of the three levels of analysis (dashed lines indicate the one to one slope) and (right) the corresponding elevation profile along the 120 m lateral survey transect. (a and b) Level 1 was a nearest-neighbor comparison of LiDAR versus surveyed ground elevations. (c and d) Level 2 was a comparison of surveyed spot heights with the nearest elevation value from a 2 m interpolated DEM. (e and f) Level 3 was a comparison of elevations derived from interpolating both the LiDAR ground returns and the surveyed ground returns to a 2 m resolution DEM. Note the scatterplots include all points collected within the wetland margins, whereas the profiles are only those along the lateral transect.

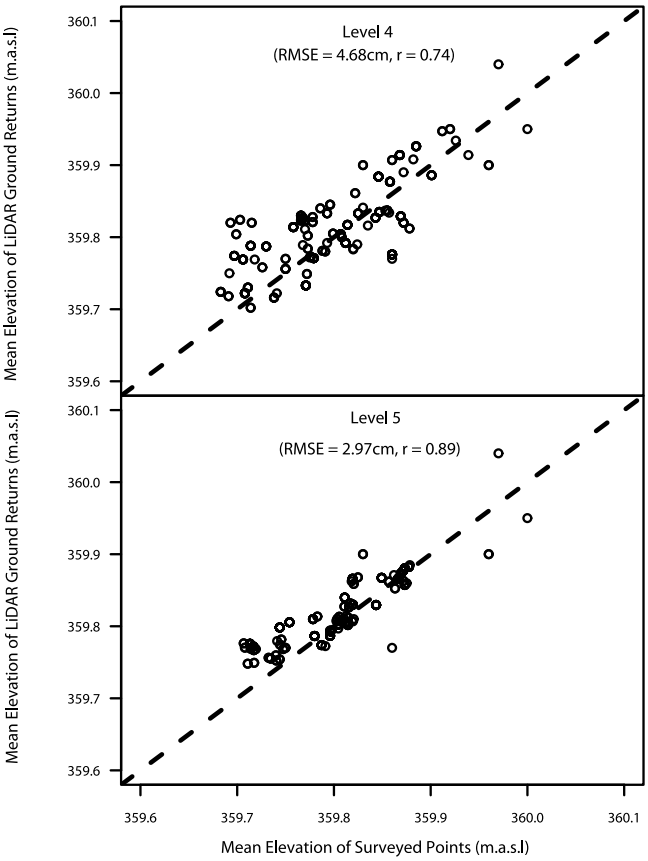


**Figure 5.** Results of LiDAR accuracy assessment for PC1 wetland in the Muskoka-Haliburton region (levels 4 and 5). These two levels compare the mean elevations of clusters (n = 10 for level 4 and n = 25 for level 5) of spatially contiguous LiDAR ground returns and surveyed spot heights.

in the running means for the chemistry data up to the LiDAR derived lagg width. At L658 however, MeHg concentrations increased first, and then declined rapidly up to the LiDAR-derived LWI distance. Standard deviation also decreased up to the LWI distance at all sites, although the trend was not as strong at the L658 wetland. In all cases there was also a noticeable, but generally small, increase in the running means within a short distance past the lagg width. At S2 and S6 wetlands this trend was more pronounced and mirrored by the standard deviation as well. Overall, the S2 wetland results were somewhat anomalous relative to the other three sites, with the highest MeHg concentrations occurring not in the wetland marginal areas but in the central domed area instead. However, the initial decrease in MeHg mean and standard deviation with increasing distance from the peatland margin was still consistent with the other 3 sites. MeHg concentrations were also significantly lower at this site compared to the other three sites (note differences in *y* axis scales in Figures 7a–7d, running means and standard deviations).

### 4.3. Correlations Between Wetland Geomorphic Indices and Topographic Setting

[34] There were strong relationships between the wetland scale geomorphic indices used to quantify their characteristic morphologies (LWI and LSI) and several of the landscape indices used to describe their topographic setting, primarily for the two composite indices, $PTI_1$ and $PTI_2$ (Table 1). The relationships were weak to nonexistent for most of the landscape indices comprising these composite indices, when considered on an individual basis. There was, however, a significant relationship between upslope contributing area and both LWI ($r^2 = 0.43$, $p < 0.001$) and LSI ($r^2 = 0.29$, $p < 0.05$). Normalizing upland area by wetland area or perimeter did not improve these relationships however. There was no significant relationship between either of the two indices (LWI and LSI) and tan $\alpha_{1m}$. The composite indices, $PTI_1$ and in particular $PTI_2$, explained a significant proportion of the variability in both the LSI and LWI (Figure 8). A negative power law function described the relationship between LSI and $PTI_2$ ($r^2 = 0.65$, $p < 0.001$) whereas LWI was positively and linear correlated with $PTI_2$ ($r^2 = 0.58$, $p < 0.001$).

## 5. Discussion

[35] Physical processes governing the nature and occurrence of biogeochemical hot spots in near-stream riparian areas have been studied extensively [*Burt and Pinau*, 2005; *Cirmo and McDonnell*, 1997; *Vidon and Hill*, 2004], and recent progress has also been made with respect to the incorporation of such process-based findings into landscape-scale conceptual or predictive modeling frameworks [*Baker et al.*, 2001; *McGlynn and Seibert*, 2003; *Vidon and Hill*, 2004]. With relatively few exceptions however [e.g., *Mitchell and Branfireun*, 2005; *Mitchell et al.*, 2008b] comparatively little research has been conducted to examine analogous processes occurring across upland-wetland ecotones, or to quantify the aggregated effects of their occurrences across scales. The current study, which details to the best of our knowledge the first attempt to correlate geomorphic patterns derived from remote sensing imagery with in situ observations of peat pore water chemistry, offers a new conceptual and methodological framework for understanding the nature and occurrence of biogeochemical hot spots in northern forested landscapes. The results imply strong potential to infer landscape-scale mechanisms giving rise to biogeochemical hot spots, such as for MeHg production, across upland-wetland interfaces.

### 5.1. LiDAR Accuracy Assessment and Derivation of Characteristic Morphologies

[36] The LiDAR accuracy assessment results (Figures 4 and 5) indicated that the gradient-analysis approach depicted in Figure 3b can be used to objectively and accurately quantify the characteristic morphologies of wetlands (i.e., LWI or average lagg width, and LSI which is a proxy for the degree of convexity or dome shape of the wetland). While the observed, mesoscale topographic gradients were very subtle, on the order of 0.2% to 1%, the LiDAR accuracy assessment confirmed that with moderate spatial aggregation of ground returns, very small differences in mean elevations, on the order of 3 cm or less, could be accurately quantified. This is considerably better than a RMSE of 7.5 cm which is the absolute accuracy typically reported by LiDAR service providers. While aggregation of the ground return elevations (i.e., taking spatial averages or

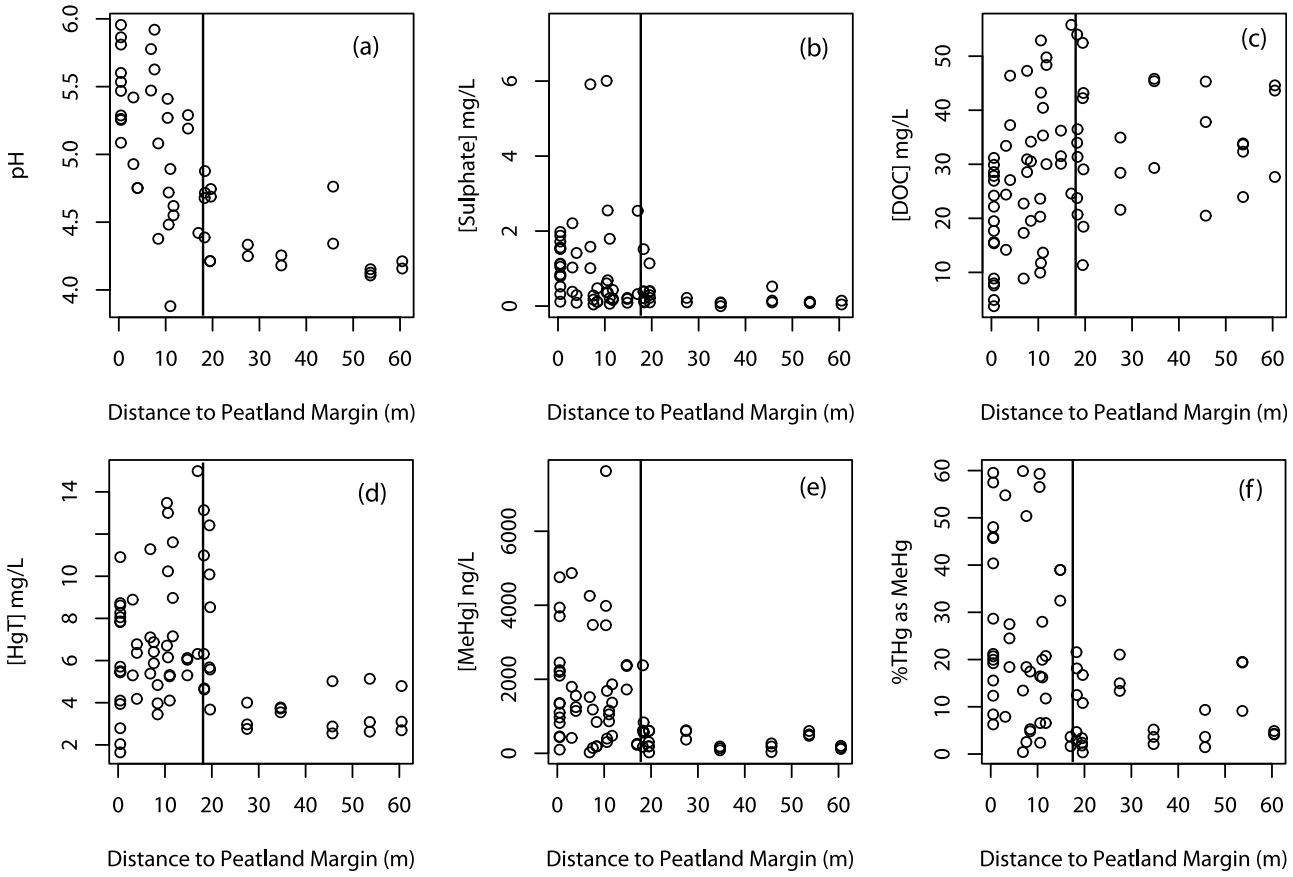


**Figure 6.** Scatterplots of various pore water chemical parameters as a function of distance to wetland margin at L239 wetland, ELA, from the August sampling campaign. (a) pH, (b) sulfate, (c) DOC, (d) HgT, (e) MeHg, and (f) %THg as MeHg. Vertical solid lines demarcate the LiDAR-derived Lagg Width Index (LWI).

interpolating) decreased the range of observations as seen in Figures 4 and 5, the means were very well preserved. The characteristic morphologies reported here therefore represent actual, but very subtle differences (on the order of 5–15 cm) in the average ground surface elevations between the peripheral and central areas of the wetlands. Airborne LiDAR is currently the only available source of topographic data that are sufficiently detailed, accurate and extensive to permit such a fine-scale analysis of forested wetland morphologies at the landscape scale.

### 5.2. Correlation Between LiDAR-Derived Geomorphic Gradients and Pore Water Chemistry: Indicators of MeHg Hot Spots in Northern Forested Wetlands

[37] Geomorphic gradients frequently give rise to strong ecological gradients, and provide a means to link landscape patterns to ecological processes of interest. Our analysis of previously published pore water chemistry data illustrates that hot spots of net MeHg production and/or accumulation (MeHg hot spots) are spatially coincident with LiDAR-derived geomorphic features, namely the lagg areas. The LWI may therefore be a good indicator of the occurrence and spatial extent of MeHg hot spots across upland-wetland interfaces in northern forested landscapes. This analysis and conclusion is based on the principle that spatial nonstationarity (spatial nonuniformity in mean and variance of a sample population) is indicative of an external force acting to produce the observed ecological phenomenon, a concept widely used by landscape ecologists [*Fortin and Dale*, 2005] The running means and standard deviations for the pore water MeHg concentrations clearly depict spatial nonstationarity. MeHg concentrations tended to be highest within the LiDAR derived lagg area and decreased rapidly up to the LWI distance, most likely in response to the decreasing influence of upslope inputs. Furthermore, clear inflections in the running means and standard deviations occurred at or very close to the LWI (Figure 7). These observations were most noticeable at the L239 wetland, but were also apparent at the other three sites, although at S2 the running means and standard deviations were actually highest in the central dome area.

[38] Several studies have illustrated the importance of upslope hydrological and biogeochemical inputs to subsurface reduction-oxidation conditions and pore water chemistry [*Heyes et al.*, 2000; *Mitchell and Branfireun*, 2005; *Mitchell et al.*, 2009]. Other experimental research has shown that peatland pore water MeHg concentrations can be artificially increased by stimulating microbial respiration (namely of sulfate reducing bacteria) through in situ additions of sulfate and/or labile organic carbon [*Jeremiason et al.*, 2006; *Mitchell et al.*, 2008a]. Upland-wetland interactions are therefore a plausible source of the spatial nonstationarity

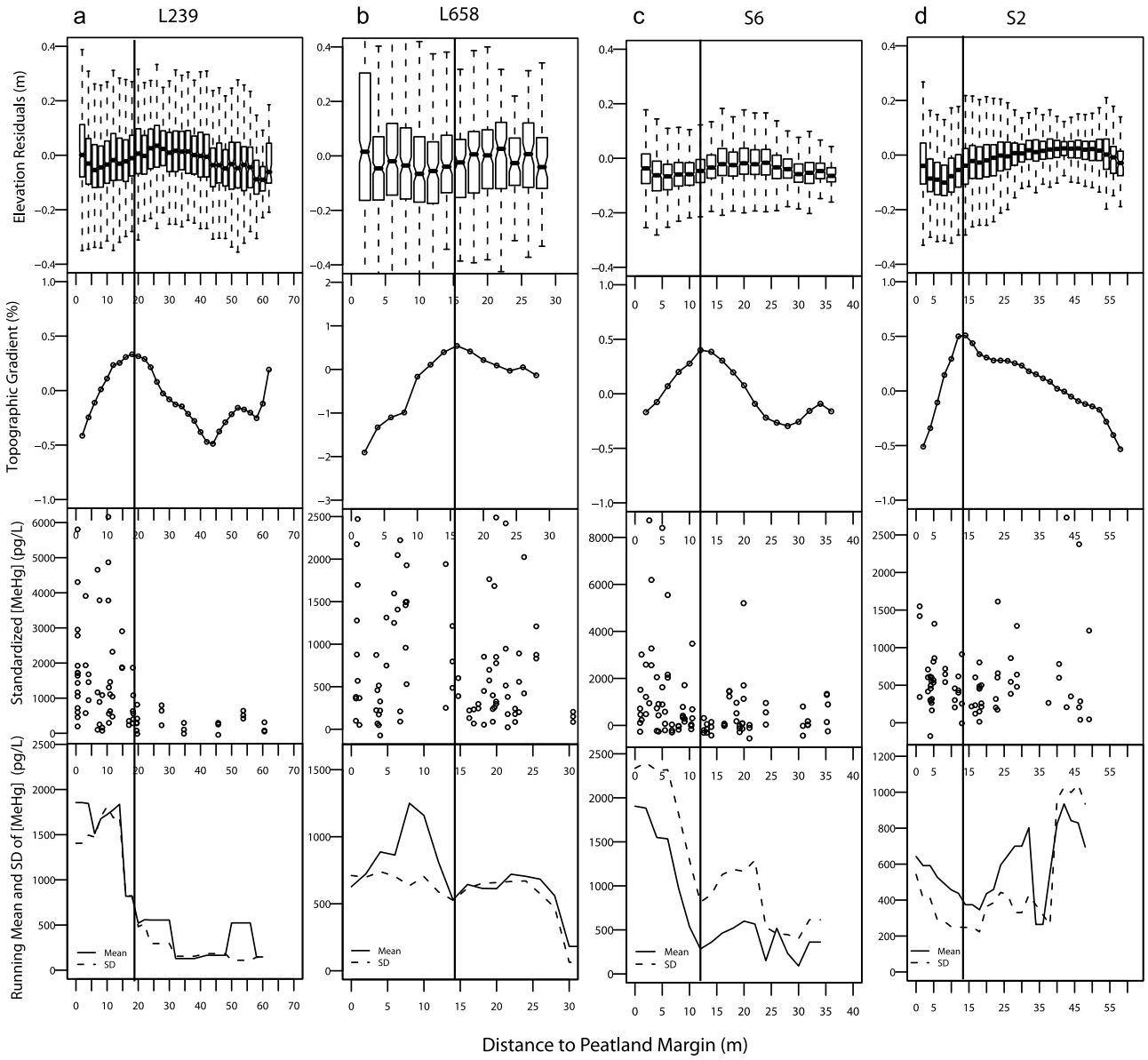


**Figure 7.** Correlation between LiDAR-derived lagg widths (vertical lines) and standardized MeHg concentrations at (a) L239, (b) L658, (c) S6, and (d) S2 wetland sites. The running mean (solid line) and standard deviation (dashed line) of the chemistry data were computed based on a 8 m moving window, computed at 2 m increments extending from the wetland edge to wetland center (as seen in Figure 2d).

observed in Figure 7, at least in the peripheral lagg area defined by the LWI [*Mitchell et al.*, 2008a, 2008b]. The correlations between this LiDAR-derived geomorphic feature and subsurface concentrations of MeHg therefore implies that the index could be used to stratify sampling regimes and extrapolate point-scale observations of wetland pore water chemistry, which are notoriously heterogeneous, particularly with respect to MeHg [*Branfireun*, 2004].

[39] Spatial nonstationarity of pore water variables was most pronounced within the LiDAR derived lagg area, and the break in the statistical properties clearly coincided with the LWI at all sites. However, spatial nonstationarity was also observed somewhat consistently, but to varying degrees, within the central dome regions of the wetlands, particularly at S2. This suggests that other processes, possibly independent from upland-wetland interactions, also influenced the subsurface biogeochemical environment. In particular, at all sites there was a consistent, abrupt increase in the running mean of concentration z scores within 5–10 m of the edge defined by LWI, toward the center of the wetland (Figure 7). The focus of this study was on biogeochemical processes at the upland-wetland interface. Further research is required to investigate other possible causes of this spatial nonstationarity such as preferential hydrologic flow paths or the possible influence of microtopographic or mesotopographic variability in governing the zone of water table fluctuations relative to the peat surface.

**Table 1.** Relationships Between Wetland Characteristic Morphologies, LSI and LWI, and Eight Geomorphic Indices Used to Describe the Topographic Setting of 14 Forested Wetlands in Muskoka-Haliburton, ELA, and MEF[a]

| Model | Equation | $r^2$ |
|---|---|---|
| LSI vs $a_{wetland}$ | $y = 20.9x - 0.39$ | 0.16 ($p = 0.165$) |
| LSI vs $a_{upslope}$ | $y = -0.57x - 0.57$ | 0.43 ($p < 0.1$) |
| LSI vs $p_{wetland}$ | $y = -1.29*10^{-0.4}x + 0.51$ | 0.21 ($p < 0.1$) |
| LSI vs $a_{upslope}$:$a_{wetland}$ | $y = 0.66x^{-0.60}$ | 0.39 ($p < 0.01$) |
| LSI vs $a_{upslope}$:$p_{wetland}$ | $y = 5.93x^{-0.61}$ | 0.48 ($p < 0.01$) |
| LSI vs $\alpha_{1m}$ | $y = 0.45x + 0.12$ | 0.14 ($p = 0.188$) |
| LSI vs $PTI_1$ | $y = 1.18x - 0.58$ | 0.61 ($p < 0.001$) |
| LSI vs $PTI_2$ | $y = 9.19x^{-0.58}$ | 0.64 ($p < 0.001$) |
| LWI vs $a_{wetland}$ | $y = 6.7*10^{-5}x + 15.4$ | 0.10 ($p = 0.142$) |
| LWI vs $a_{upslope}$ | $y = 1.75*10^{-5}x + 14.3$ | 0.29 ($p < 0.05$) |
| LWI vs $p_{wetland}$ | $y = 0.004x + 11.7$ | 0.19 ($p < 0.05$) |
| LWI vs $a_{upslope}$:$a_{wetland}$ | $y = 0.58x + 16.7$ | 0.02 ($p = 0.295$) |
| LWI vs $a_{upslope}$:$p_{wetland}$ | $y = 0.02x + 14.8$ | 0.1 ($p = 0.14$) |
| LWI vs $\alpha_{1m}$ | $y = -18x + 26.6$ | 0.11 ($p = 0.131$) |
| LWI vs $PTI_1$ | $y = 0.53x + 11.6$ | 0.57 ($p < 0.001$) |
| LWI vs $PTI_2$ | $y = 0.01x + 11.79$ | 0.58 ($p < 0.001$) |

[a]LSI, lateral slope index; LWI, lagg width index. Relationships with $PTI_1$ and $PTI_2$, which are composite indices relating upslope area:wetland area ($PTI_1$), upslope area:wetland perimeter ($PTI_2$), and wetland drainage conditions, are highly significant despite poor or absent relationships with their component indices when considered on an individual basis.

### 5.3. Influence of Topographic Setting on Characteristic Morphologies of Northern Forested Wetlands: Toward a Scaling Framework

[40] The surface topography of a wetland provides insight into its dominant sources of water, and potentially also into the subsurface biogeochemical conditions affecting nutrient/contaminant transformations and transport within its margins [*Damman*, 1986].

[41] The ability to quantify characteristic morphologies of forested wetlands with LiDAR ground surface topography therefore offers a new technique for inferring the degree of connectivity between uplands and wetlands in northern forested landscapes. Our finding that characteristic morphologies of northern forested wetlands are systematically linked to topographic setting therefore also offers new insight into the structure and function of northern forested wetlands. It corroborates the central role of hydrology in controlling the form and function of wetlands, a concept that is widely accepted within the wetland science community [*Bridgham et al.*, 1996; *Mitsch and Gosselink*, 2000]. Digital terrain analysis of characteristic morphologies therefore offers a potential strategy to improve the functional characterization of forested wetlands, particularly with respect to their influence on downstream surface water chemistry.

[42] The fourteen forested wetland sites analyzed in this study defy simple categorization using existing wetland classification schemes. Given that they are all disconnected from regional groundwater systems, hydrologic contributions from upland runoff or transient, shallow groundwater systems may be one of the most critical variables influencing the structure and function of these wetlands. However, the most widely accepted conceptual model for understanding hydrogeomorphic influences on wetland biogeochemistry in the Muskoka-Haliburton region is based on the influence of overburden thickness on the temporal persistence of upland-wetland hydrologic connectivity and hence water table elevations during periods of drought [*Devito and Hill*, 1997]. This conceptual framework does not consider the role of upslope nutrient delivery to wetlands as a factor influencing the subsurface biogeochemical conditions. A classification system that incorporates the influence of topographic setting on the supply of electron acceptors reaching wetlands may improve our ability to discriminate wetlands on the basis of their functional characteristics, particularly with respect to carbon, sulfur, and mercury cycling.

[43] The geomorphic evolution of northern forested wetlands reflects the influence of topographic setting on their hydrology and subsurface biogeochemical environment, and may form the basis for such a classification system. Lagg areas represent a discrete zone of enhanced upland-wetland interaction, reflecting the spatially varying influence of upslope inputs on rates of peat degradation caused by inputs of dissolved oxygen and other electron acceptors such as sulfate [*Schiff et al.*, 1998]. Hydrological and biogeochemical conditions within the lagg area are therefore strongly

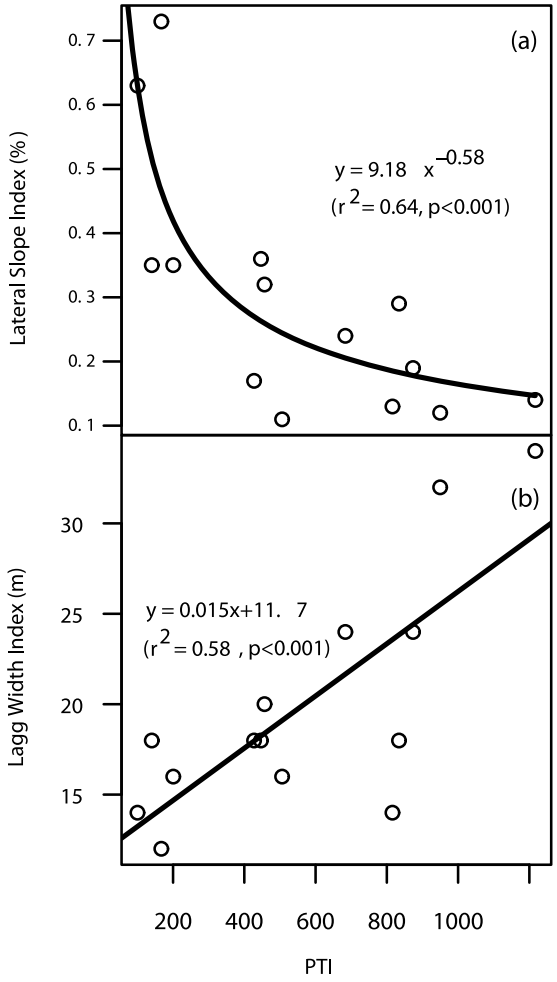


**Figure 8.** Correlation between the quantitative geomorphic indices describing characteristic morphologies of 14 forested wetlands and $PTI_2$, an index describing topographic setting as a function of upslope contributing area, wetland geometry, and local drainage conditions. (a) Lateral slope index and (b) lagg width index.

influenced by upslope contributing areas. For example, *Waddington et al.* [2005] observed peat degradation and lagg expansion around the margins of a kettle hole peatland in southern Ontario in response to a period of agricultural intensification in the surrounding catchment. Surface convexity is also an indicator of ombrotrophy and moisture availability in wetlands [*Damman*, 1986]. The characteristic morphology analysis illustrated in Figure 3 provides an estimate of the spatial extents of lagg and dome features in forested wetlands, thus providing insight into factors influencing their geomorphic evolution. While peatland development is a complicated process that is beyond the scope of this study, the systematic occurrence of a lagg zone around the wetland margins leading gradually to a raised plateau at or near the wetland center across all sites, is strong evidence of autogenic peatland development processes [*Bridgham et al.*, 1996]. The morphology of forested wetlands is therefore probably indicative of the spatially varying influence of upslope hydrological and biogeochemical inputs and the natural successional development of basin wetlands over many thousands of years as influenced by their topographic setting and local drainage conditions.

[44] The PTI indices are analogous to the $\ln(a/\tan\beta)$ index of *Beven and Kirkby* [1979] aggregated to the scale of individual landscape units. They account for upslope contributing area per unit wetland area ($PTI_1$) or perimeter ($PTI_2$) as well as local drainage conditions. Figure 8 illustrates that as the ratio of upslope contributing area to peatland perimeter increases, and/or the slope of the wetland surface decreases (implying less efficient drainage), the relative "openness" of a wetland to upland hydrological and biogeochemical inputs increases. This is manifested as a wider lagg area and a more subdued (less convex) dome shape (as inferred from the LSI). The correlation between the LiDAR-derived lagg width and elevated pore water concentrations of MeHg concentrations (Figure 7) further suggests that increasing values of PTI results in a greater incursion of upslope inputs, and hence a greater influence of upslope areas on the subsurface biogeochemical environment. Because of the strong correlation between lagg width and $PTI_2$, there exists the potential to predict lagg areas within individual wetlands based on simple geomorphic indices such as upslope area, wetland area, wetland perimeter and wetland slope. This would simplify the quantification of lagg areas over large regions although it has yet to be determined whether or not LiDAR DEMs are the only source of topographic data that will permit these types of analyses.

[45] It remains unclear how upland-wetland interactions influence downstream water chemistry at the landscape scale, especially in relation to MeHg. Many studies have identified wetlands as a critical factor governing stream water, lake sediment, and -fish tissue concentrations of MeHg [*Balogh et al.*, 2005; *Hurley et al.*, 1995; *Scherbatskoy et al.*, 1998; *Shanley et al.*, 2005; *Wiener et al.*, 2006]. Compared to other water quality parameters these correlations are typically weak. For example, wetland areas derived from LiDAR DEMs has been shown to explain close to 95% of the variability in landscape DOC export in regression models applied to the Algoma-Highlands [*Creed et al.*, 2003] and Muskoka-Haliburton regions [*Richardson et al.*, 2009] of Ontario. The nature of MeHg production in wetlands is such that that the delivery of electron acceptors from upslope areas, primarily sulfate, is likely a limiting factor in dictating the MeHg source-strength potential of individual wetlands [*Mitchell et al.*, 2008b, 2009]. The correlation between LWI and PTI suggests that lagg areas, which are also considered to be important hydrological source areas [*Urban et al.*, 1989], can be effectively mapped at the landscape scale using easily derived metrics describing topographic setting, including wetland contributing areas, wetland geometry, and local drainage conditions. Specific information on lagg areas could then be used to structure and test hypotheses related to the nature, occurrence and relevance of MeHg or other biogeochemical hotpots at the landscape scale. Although we do not currently have water quality data from a sufficiently broad range of study sites, we hypothesize that the PTI index introduced here would be directly related to how well biogeochemical hot spots at the upland-wetland interface are translated to downstream surface water concentrations of MeHg.

## 6. Conclusions

[46] Prior to the availability of high-resolution LiDAR surveys, observing subtle topographic gradients within wetland environments was virtually impossible, thus precluding mechanistic linkages between geomorphic patterns and ecological processes. This study demonstrates the unprecedented ability to characterize the geomorphic form of northern forested wetlands using high-resolution digital topography from airborne LiDAR. The results emphasize the influence of upslope contributing area and local drainage conditions as a critical factor influencing the geomorphology and subsurface hydrochemistry of northern forested wetlands that are disconnected from regional groundwater systems. Strong spatial agreement between LiDAR-derived geomorphic gradients, and the spatial extent of biogeochemical hot spots of MeHg production and/or accumulation in four intensively studied wetlands was illustrated. Moreover, two quantitative geomorphic indices describing the lagg width and the lateral slope of the characteristic dome shape of the wetland surface were strongly correlated with topographic setting. This implies that easily quantified metrics describing the topographic setting of individual wetlands, including upslope contributing area, wetland geometry (area and perimeter) and local drainage conditions, might be useful for inferring some fundamental structural, functional, and even biogeochemical characteristics of wetlands at the landscape scale. It also provides new evidence suggesting that topographic setting influences the geomorphological evolution of forested wetlands, a phenomenon that was hitherto unobservable because of a lack of sufficiently detailed and accurate topographic information. Overall, this study demonstrates the enticing potential to use digital terrain analysis of airborne LiDAR surveys covering large geographic regions to characterize ecosystem functions of forested wetlands and to investigate the nature, occurrence and relevance of biogeochemical hot spots across upland-wetland interfaces in northern forested landscapes.

[47] **Acknowledgments.** We gratefully acknowledge financial support for this research from the Natural Sciences and Engineering Research Council in the form a NSERC CGS to MCR and a NSERC discovery grant

to BAB. We would also like to thank Chris Hopkinson and Laura Chasmer of the Applied Geomatics Research Group for conducting the LIDAR surveys at the Muskoka-Haliburton sites.

## References


Baker, M. E., M. J. Wiley, and P. W. Seelbach (2001), GIS-based hydrologic modeling of riparian areas: Implications for stream water quality, *J. Am. Water Resour. Assoc.*, *37*(6), 1615–1628, doi:10.1111/j.1752-1688.2001.tb03664.x.

Balogh, S. J., Y. H. Nollet, and H. J. Offerman (2005), A comparison of total mercury and methylmercury export from various Minnesota watersheds, *Sci. Total Environ.*, *340*(1–3), 261–270, doi:10.1016/j.scitotenv.2004.08.013.

Beven, K. J., and M. J. Kirkby (1979), A physically based, variable contributing area model of basin hydrology, *Hydrol. Sci. Bull.*, *24*(1), 43–69, doi:10.1080/02626667909491834.

Branfireun, B. A. (2004), Does microtopography influence subsurface pore-water chemistry? Implications for the study of methylmercury in peatlands, *Wetlands*, *24*(1), 207–211, doi:10.1672/0277-5212(2004)024[0207:DMISPC]2.0.CO;2.

Branfireun, B. A., A. Heyes, and N. T. Roulet (1996), The hydrology and methylmercury dynamics of a Precambrian Shield headwater peatland, *Water Resour. Res.*, *32*(6), 1785–1794, doi:10.1029/96WR00790.

Bridgham, S. D., J. Pastor, J. A. Janssens, C. Chapin, and T. J. Malterer (1996), Multiple limiting gradients in peatlands: A call for a new paradigm, *Wetlands*, *16*(1), 45–65, doi:10.1007/BF03160645.

Burt, T. P., and G. Pinau (2005), Linking hydrology and biogeochemistry in complex landscapes, *Prog. Phys. Geogr.*, *29*(3), 297–316, doi:10.1191/0309133305pp450ra.

Cirmo, C. P., and J. J. McDonnell (1997), Linking the hydrologic and biogeochemical controls of nitrogen transport in near-stream zones of temperate-forested catchments: A review, *J. Hydrol.*, *199*(1–2), 88–120, doi:10.1016/S0022-1694(96)03286-6.

Creed, I. F., S. E. Sanford, F. D. Beall, L. A. Molot, and P. J. Dillon (2003), Cryptic wetlands: Integrating hidden wetlands in regression models of the export of dissolved organic carbon from forested landscapes, *Hydrol. Process.*, *17*(18), 3629–3648, doi:10.1002/hyp.1357.

Damman, A. W. H. (1986), Hydrology, development, and biogeochemistry of ombrogenous peat bogs with special reference to nutrient relocation in a western Newfoundland bog, *Can. J. Bot.*, *64*(2), 384–394, doi:10.1139/b86-055.

Devito, K. J., and A. R. Hill (1997), Sulphate dynamics in relation to groundwater-surface water interactions in headwater wetlands of the southern Canadian Shield, *Hydrol. Process.*, *11*(5), 485–500, doi:10.1002/(SICI)1099-1085(199704)11:5<485::AID-HYP455>3.0.CO;2-F.

Devito, K. J., and A. R. Hill (1999), Sulphate mobilization and pore water chemistry in relation to groundwater hydrology and summer drought in two conifer swamps on the Canadian Shield, *Water Air Soil Pollut.*, *113*, 97–114, doi:10.1023/A:1005081505086.

Devito, K. J., A. R. Hill, and P. J. Dillon (1999), Episodic sulphate export from wetlands in acidified headwater catchments: Prediction at the landscape scale, *Biogeochemistry*, *44*(2), 187–203, doi:10.1007/BF00992978.

Dillon, P. J., and L. A. Molot (1997), Effect of landscape form on export of dissolved organic carbon, iron and phosphorous from forested stream catchments, *Water Resour. Res.*, *33*(11), 2591–2600, doi:10.1029/97WR01921.

Florinsky, I. V., S. McMahon, and D. L. Burton (2004), Topographic control of soil microbial activity: A case study of denitrifiers, *Geoderma*, *119*(1–2), 33–53, doi:10.1016/S0016-7061(03)00224-6.

Fortin, M. J., and M. R. T. Dale (2005), *Spatial Analysis: A Guide for Ecologists*, 365 pp., doi:10.1017/CBO9780511542039, Cambridge Univ. Press, Cambridge, U. K.

Heyes, A., T. R. Moore, J. W. M. Rudd, and J. J. Dugoua (2000), Methyl mercury in pristine and impounded boreal peatlands, experimental Lakes Area, Ontario, *Can. J. Fish. Aquat. Sci.*, *57*(11), 2211–2222, doi:10.1139/cjfas-57-11-2211.

Hjerdt, K. N., J. J. McDonnell, J. Seibart, and A. Rodhe (2004), A new topographic index to quantify the downslope controls on local drainage, *Water Resour. Res.*, *40*, W05602, doi:10.1029/2004WR003130.

Hopkinson, C., L. E. Chasmer, G. Sass, I. F. Creed, M. Sitar, W. Kalbfleisch, and P. Treitz (2005), Vegetation class dependent errors in lidar ground elevation and canopy height estimates in a boreal wetland environment, *Can. J. Remote Sens.*, *31*(2), 191–206.

Hurley, J. P., J. P. Benoit, C. L. Babiarz, M. M. Shafer, A. W. Andren, J. R. Sullivan, R. Hammond, and D. A. Webb (1995), Influences of watershed characteristics on mercury levels in Wisconsin rivers, *Environ. Sci. Technol.*, *29*(7), 1867–1875, doi:10.1021/es00007a026.

Jencso, K. G., B. L. McGlynn, M. N. Gooseff, S. M. Wondzell, K. E. Bencala, and L. A. Marshall (2009), Hydrologic connectivity between landscapes and streams: Transferring reach-and plot-scale understanding to the catchment scale, *Water Resour. Res.*, *45*, W04428, doi:10.1029/2008WR007225.

Jeremiason, J. D., D. R. Engstrom, E. B. Swain, E. A. Nater, B. M. Johnson, J. E. Almendinger, B. A. Monson, and R. K. Kolka (2006), Sulfate addition increases methylmercury production in an experimental wetland, *Environ. Sci. Technol.*, *40*(12), 3800–3806, doi:10.1021/es0524144.

Jones, K. L., G. C. Poole, S. J. O'Daniel, L. A. K. Mertes, and J. A. Stanford (2008), Surface hydrology of low-relief landscapes: Assessing surface water flow impedance using LIDAR-derived digital elevation models, *Remote Sens. Environ.*, *112*(11), 4148–4158, doi:10.1016/j.rse.2008.01.024.

Kolka, R. K., D. F. Grigal, E. A. Nater, and E. S. Verry (2001), Hydrologic cycling of mercury and organic carbon in a forested upland-bog watershed, *Soil Sci. Soc. Am. J.*, *65*(3), 897–905.

MacMillan, R. A., T. C. Martin, T. J. Earle, and D. H. McNabb (2003), Automated analysis and classification of landforms using high-resolution digital elevation data: Applications and issues, *Can. J. Remote Sens.*, *29*(5), 592–606.

McClain, M. E., et al. (2003), Biogeochemical hotspots and hot moments at the interface of terrestrial and aquatic ecosystems, *Ecosystems*, *6*, 301–312, doi:10.1007/s10021-003-0161-9.

McGlynn, B. L., and J. Seibert (2003), Distributed assessment of contributing area and riparian buffering along stream networks, *Water Resour. Res.*, *39*(4), 1082, doi:10.1029/2002WR001521.

Mitchell, C. P. J., and B. A. Branfireun (2005), Hydrogeomorphic controls on reduction-oxidation conditions across boreal upland-peatland interfaces, *Ecosystems*, *8*(7), 731–747, doi:10.1007/s10021-005-1792-9.

Mitchell, C. P. J., B. A. Branfireun, and R. K. Kolka (2008a), Assessing sulfate and carbon controls on net methylmercury production in peatlands: An in situ mesocosm approach, *Appl. Geochem.*, *23*(3), 503–518, doi:10.1016/j.apgeochem.2007.12.020.

Mitchell, C. P. J., B. A. Branfireun, and R. K. Kolka (2008b), Spatial characteristics of net methylmercury production hot spots in peatlands, *Environ. Sci. Technol.*, *42*(4), 1010–1016, doi:10.1021/es0704986.

Mitchell, C. P. J., B. A. Branfireun, and R. K. Kolka (2009), Methylmercury dynamics at the upland-peatland interface: Topographic and hydrogeochemical controls, *Water Resour. Res.*, *45*, W02406, doi:10.1029/2008WR006832.

Mitsch, W. J., and J. G. Gosselink (2000), *Wetlands*, 3rd ed., 920 pp., John Wiley, New York.

Munthe, J., R. A. Brodaly, B. A. Branfireun, C. T. Driscoll, C. C. Gilmour, R. Harris, M. Horvat, M. Lucotte, and O. Malm (2007), Recovery of mercury-contaminated fisheries, *Ambio*, *36*(1), 33–44, doi:10.1579/0044-7447(2007)36[33:ROMF]2.0.CO;2.

R Development Core Team (2008), R: A language and environment for statistical computing, R Found. for Stat. Comput., Vienna, Austria.

Reid, R. A., R. Girard, and A. C. Nicolls (1987), Morphometry and catchment areas for the calibrated watersheds, *Data Rep. DA 87/4*, Dorset Environ. Sci. Cent., Ont. Minist.of the Environ., Dorset, Ont., Canada.

Richardson, M. C., B. A. Branfireun, V. B. Robinson, and P. A. Graniero (2007), Towards simulating biogeochemical hot spots in the landscape: A geographic object-based approach, *J. Hydrol.*, *342*(1–2), 97–109, doi:10.1016/j.jhydrol.2007.05.016.

Richardson, M. C., M. J. Fortin, and B. A. Branfireun (2009), Hydrogeomorphic edge-detection and delineation of landscape functional units from LIDAR DEMs, *Water Resour. Res.*, *45*, W10441, doi:10.1029/2008WR007518.

Scherbatskoy, T., J. B. Shanley, and G. J. Keeler (1998), Factors controlling mercury transport in an upland forested catchment, *Water Air Soil Pollut.*, *105*, 427–438, doi:10.1023/A:1005053509133.

Schiff, S., R. Aravena, E. Mewhinney, R. Elgood, B. Warner, P. Dillon, and S. Trumbore (1998), Precambrian shield wetlands: Hydrologic control of the sources and export of dissolved organic matter, *Clim. Change*, *40*(2), 167–188, doi:10.1023/A:1005496331593.

Scull, P., J. Franklin, O. A. Chadwick, and D. McArthur (2003), Predictive soil mapping: A review, *Prog. Phys. Geogr.*, *27*(2), 171–197, doi:10.1191/0309133303pp366ra.

Shanley, J. B., N. C. Kamman, T. A. Clair, and A. Chalmers (2005), Physical controls on total and methylmercury concentrations in streams and lakes of the northeastern USA, *Ecotoxicology*, *14*(1–2), 125–134, doi:10.1007/s10646-004-6264-z.

Sonnentag, O., J. M. Chen, N. T. Roulet, W. Ju, and A. Govind (2008), Spatially explicit simulation of peatland hydrology and carbon dioxide exchange: Influence of mesoscale topography, *J. Geophys. Res.*, *113*, G02005, doi:10.1029/2007JG000605.

St. Louis, V. L., J. W. M. Rudd, C. A. Kelly, K. G. Beaty, N. S. Bloom, and R. J. Flett (1994), Importance of wetlands as sources of methyl mercury to boreal forest ecosystems, *Can. J. Fish. Aquat. Sci.*, *51*(5), 1065–1076, doi:10.1139/f94-106.

Timmons, D. R., E. S. Verry, R. E. Burwell, and R. F. Holt (1977), Nutrient transport in surface runoff and interflow from an aspen-birch forest, *J. Environ. Qual.*, *6*, 188–192.

Toyra, J., and A. Pietroniro (2005), Towards operational monitoring of a northern wetland using geomatics-based techniques, *Remote Sens. Environ.*, *97*(2), 174–191, doi:10.1016/j.rse.2005.03.012.

Urban, N. R., S. E. Bayley, and S. J. Eisenreich (1989), Export of dissolved organic carbon and acidity from peatlands, *Water Resour. Res.*, *25*(7), 1619–1628, doi:10.1029/WR025i007p01619.

Vidon, G. F., and A. R. Hill (2004), Landscape controls on the hydrology of stream riparian zones, *J. Hydrol.*, *292*, 210–228, doi:10.1016/j.jhydrol.2004.01.005.

Waddington, J. M., M. J. T. Heywood, B. D. Crosbie, and E. C. Dowsett (2005), Potential ecohydrological controls on peat degradation and vegetation pattern change in a kettle-hole bog, in *Dynamics and Biogeochemistry of River Corridors and Wetlands*, edited by L. Heathwaite et al., pp. 130–138, Int. Assoc. of Hydrol. Sci., Foz do Iguaco, Brazil.

Webster, K. L., I. F. Creed, F. D. Beall, and R. A. Bourbonniere (2008), Sensitivity of catchment-aggregated estimates of soil carbon dioxide efflux to topography under different climatic conditions, *J. Geophys. Res.*, *113*, G03040, doi:10.1029/2008JG000707.

Wiener, J. G., B. C. Knights, M. B. Sandheinrich, J. D. Jeremiason, M. E. Brigham, D. R. Engstrom, L. G. Woodruff, W. F. Cannon, and S. J. Balogh (2006), Mercury in soils, lakes, and fish in Voyageurs National Park (Minnesota): Importance of atmospheric deposition and ecosystem factors, *Environ. Sci. Technol.*, *40*(20), 6261–6268, doi:10.1021/es060822h.

Yao, H., and M. Deveau (2009), Hydrological data for Lakes and Catchments, in *Muskoka/Haliburton* (*1978–2007*), data report, Ont. Minist. of Environ., Dorset, Ont., Canada.

B. A. Branfireun, Department of Geography, University of Toronto at Mississauga, 3359 Mississauga Rd. N., Mississauga, ON L5L 1C6, Canada.

R. K. Kolka, Northern Research Station, Forest Service, U.S. Department of Agriculture, 1831 Hwy. 169 E., Grand Rapids, MN 55744, USA.

C. P. J. Mitchell, Department of Physical and Environmental Sciences, University of Toronto at Scarborough, 1265 Military Trail, Toronto, ON M1C 1A4, Canada.

M. C. Richardson, Department of Geography and Environmental Studies, Carleton University, Ottawa, ON K1S 5B6, Canada. (murray_richardson@carleton.ca)